Supporting Information

Eng et al. 10.1073/pnas.1300569110

SI Materials and Methods

Gelatin Methacrylate Synthesis. Gelatin methacrylate (GelMA) was synthesized according to a previously published method (1, 2). Briefly, gelatin (Difco) was dissolved in PBS at a concentration of 0.1 g/mL, and 1 mL of methacrylic anhydride (Sigma) per gram of gelatin was added dropwise to the gelatin solution over 30 min. The solution was stirred, allowed to react for 1 h at 60 °C, cooled to room temperature, dialyzed with a 14-kDa cutoff against ultrapure water for 4 d, frozen, and then lyophilized.

Mechanical Testing. The modulus of fabricated gelatin methacrylate gels were measured for 5%, 10%, 15%, and 20% (wt/vol) hydrogels. The equilibrium compressive Young's modulus ($n = 4$) was determined at under unconfined compression under wet conditions using a modification of an established protocol (3). An initial tare load of 0.2 N was applied followed by a stress–relaxation step where specimens were compressed at a ramp velocity of 1% per second up to 10% strain and maintained at the position for 1,800 s. The elastic modulus was obtained from the equilibrium forces measured at 10% strain, plotted as a function of hydrogel composition (percentage GelMA), and fit to a power law in Microsoft Excel.

Cardiac Contraction Analysis. The effect of shape geometry on cell function was evaluated by encapsulating cardiac myocytes in rectangular shapes with two different aspect ratios: long rectangles (1:10) and short rectangles (1:3). Shapes with encapsulated cells were cultured for 1 wk in DMEM. Video analysis was performed to determine the frequency and amplitude of macroscopic contractions. The amplitude of contractions was measured using ImageJ software, by finding the minimum and maximum distance between fixed points on the two ends of the cardiomyocyte-laden hydrogel shapes during each contraction cycle. The measured difference was calculated as a percentage of total length ($n = 50$). The frequency was measured from the number of contractions in the entire video per unit time ($n = 27$).

1. Van Den Bulcke AI, et al. (2000) Structural and rheological properties of methacrylamide modified gelatin hydrogels. *Biomacromolecules* 1(1):31–38.
2. Nichol JW, et al. (2010) Cell-laden microengineered gelatin methacrylate hydrogels. *Biomaterials* 31(21):5536–5544.
3. Mauck RL, et al. (2000) Functional tissue engineering of articular cartilage through dynamic loading of chondrocyte-seeded agarose gels. *J Biomech Eng* 122(3):252–260.

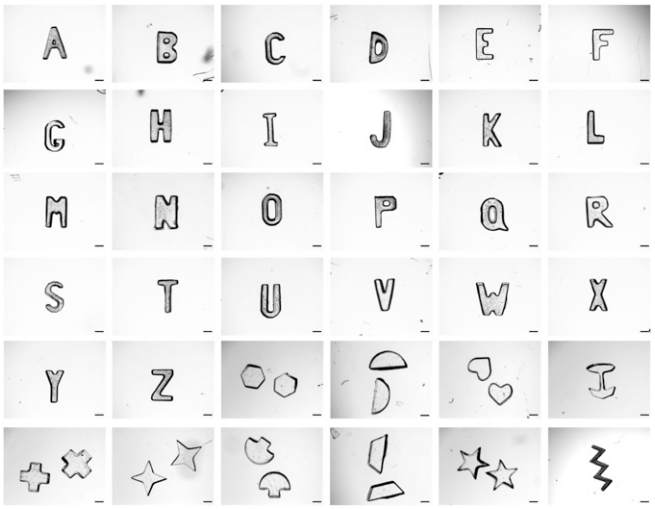

Fig. S1. A library of hydrogel shapes. Bright-field images of 36 additional shapes are shown to demonstrate potential geometries and thus species that can be patterned. The English alphabet was chosen as a simple and easily recognizable set of distinct and mutually exclusive shape geometries. These additional shapes were designed to maintain mutual exclusivity with all other shapes. If more than 36 species need to be patterned, many other shape geometries can be designed. (Scale bar: 200 μm.)

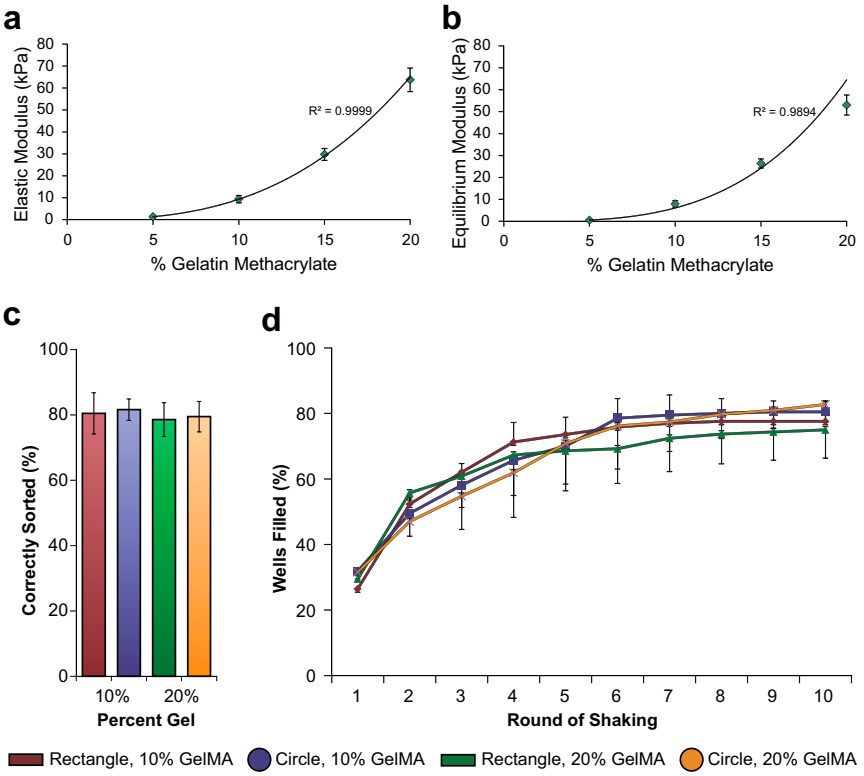

Fig. S2. Effect of different percent gelatin methacrylate (GelMA) on mechanical properties and sorting. (*A* and *B*) Mechanical testing of gelatin methacrylate hydrogels. (*A*) Elastic and (*B*) equilibrium modulus of 5%, 10%, 15%, and 20% (wt/vol) gelatin methacrylate ($n = 4$). The elastic modulus ranged from 0.5 to 53 kPa, and the equilibrium modulus ranged from 1.3 to 63 kPa. Both fit a power law with R^2 values of 0.9999 and 0.9894. (*C* and *D*) Sorting specificity and efficiency for different shapes and gel percentages. The same sorting assays as in Fig. 1 were performed using 10% and 20% (wt/vol) GelMA. (*C*) After five rounds of sorting, both 10% and 20% gels, and circles and rectangles sorted with ~80% specificity. Specificity was defined as the number of correctly docked shapes divided by the total number of docked shapes. Error bars represent SD from the mean. Two-way ANOVA comparing different gel percentages and different shape geometries yielded no significant differences between groups ($n = 3$, $P > 0.05$). (*D*) Sorting yield, the percentage of total wells in the pattern filled with congruent shapes, were plotted as a function of rounds of shaking for the four different conditions. Error bars represent the SD from the mean. Two-way ANOVA comparing different gel percentages and different shape geometries at each round of shaking yielded no significant differences between groups ($n = 3$, $P > 0.05$).

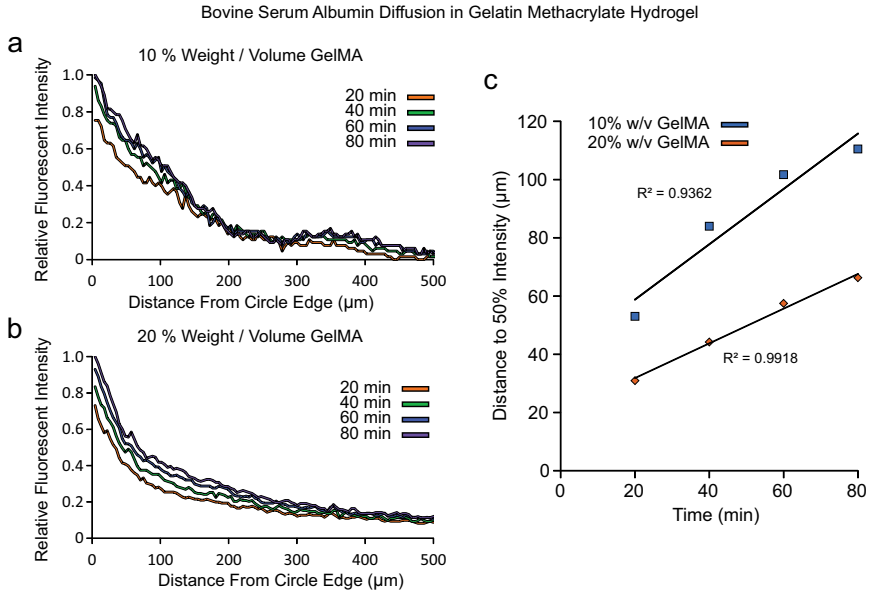

Fig. S3. Diffusion of BSA from gelatin methacrylate (GelMA) hydrogels. Circles fabricated with 10% (wt/vol) GelMA and 20% (wt/vol) GelMA were dosed with Texas Red-tagged BSA and were sorted in 10% (wt/vol) GelMA and 20% (wt/vol) GelMA, respectively. Time lapse images of sorted circles dosed with Texas Red-tagged BSA were taken at 10-min intervals for 100 min. Relative fluorescence intensity was plotted as a function of distance from the circle edge for five time points. *A* represents a plot for 10% (wt/vol) GelMA, whereas *B* represents 20% (wt/vol) BSA. (*C*) For each time point, the distance to 50% intensity was determined and plotted as a function of time. These fit a linear curve with R^2 of 0.9362 and 0.9918. The higher slope for the 10% (wt/vol) GelMA diffusion suggests a higher rate of diffusion.

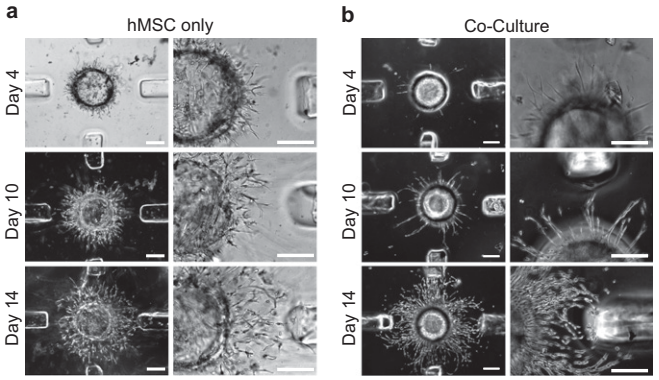

Fig. S4. Time line of mesenchymal stem cell (MSC) migration in shape-coded templates, cultured alone and with endothelial cells (ECs). (*A*) Bright-field images of the MSC monoculture after 14 d, where encapsulated MSCs migrated from the circular hydrogel through the GelMA matrix. (*B*) Bright-field images of the MSC–EC coculture, showing the progression of encapsulated MSC cell migration over 14 d from the circular hydrogel to the EC-laden rectangular hydrogels. Two magnifications are shown for both sets of images. (Scale bars: 300 μm.)

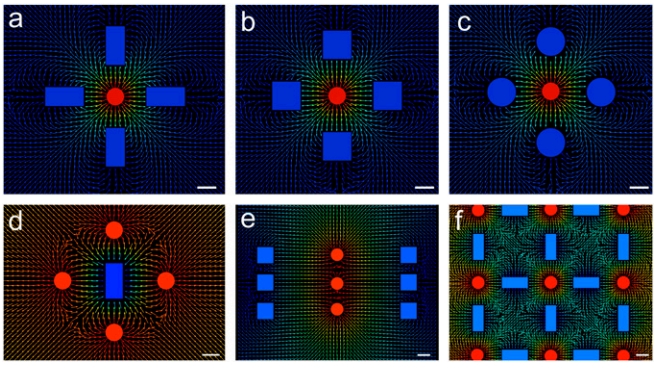

Fig. S5. Finite element modeling of concentration gradients. The colored arrows represent the relative contribution of either of the two driving forces for the resultant gradient vector, where red represents mesenchymal stem cell (MSC) outward migration as the primary driving force and blue represents endothelial cell (EC) attraction as the primary driving force. (*A*–*C*) Independence of the concentration gradient field from shape geometry. Concentration gradient profiles are shown as arrow plot with three different shape geometries for the exterior shape: (*A*) rectangles, (*B*) squares, and (*C*) circles. The same spatial arrangement as found in Figs. 2 and 3 was used to position the two different shape types in each simulation. (*D*–*F*) Dependence of the concentration gradient field on shape arrangement. Concentration gradient profiles are shown as arrow plot with three different arrangements of shapes. (*D*) Reversed shape pattern from the rectangle and circle placement found in Fig. 3, with a rectangle in the center with surrounding circles. (*E*) A linear gradient field can be created by arranging the shapes in rows. (*F*) Repeating the pattern found in Fig. 3 creates a more complex large scale gradient field. (Scale bar: 300 μm.)

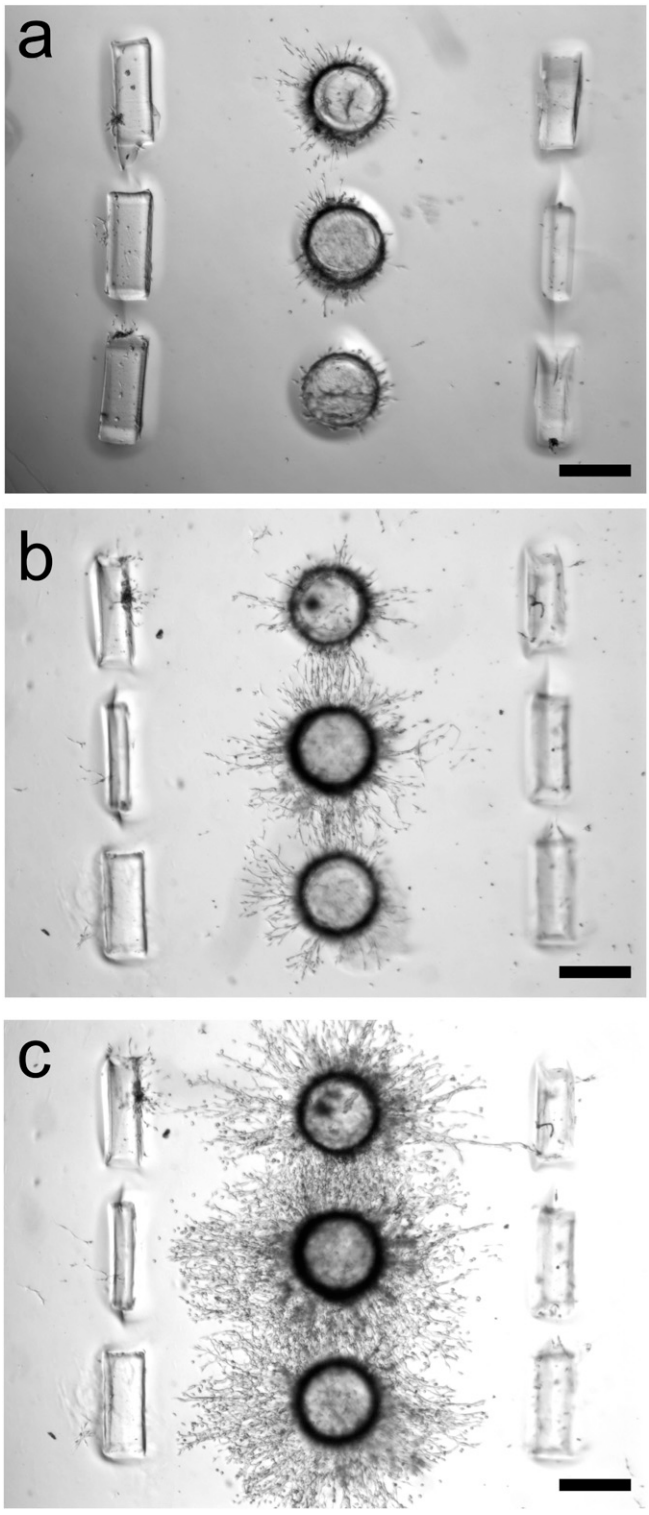

Fig. S6. Time line of mesenchymal stem cell (MSC) migration in shape-coded templates, cultured with endothelial cells (ECs). Bright-field images of MSC-EC coculture at (*A*) 4, (*B*) 10, and (*C*) 14 d, showing the progression of MSC migration over time. MSCs were encapsulated in circles, whereas ECs were encapsulated in rectangles. (Scale bars: 600 μm.)

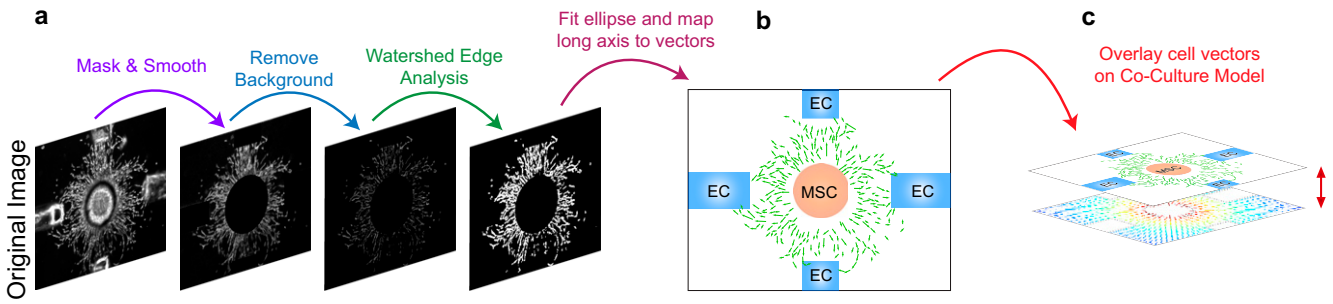

Fig. S7. Schematic of image processing. (*A*) Experimental images of migrating cells were processed using an image-processing algorithm in MATLAB to recognize each cell as a vector for quantification. (*B*) Once each image was transformed into a vector of cell data, multiple images were combined using the same relative spatial landmarks. (*C*) Finally, the vectors were compared with those generated from the finite element modeling.

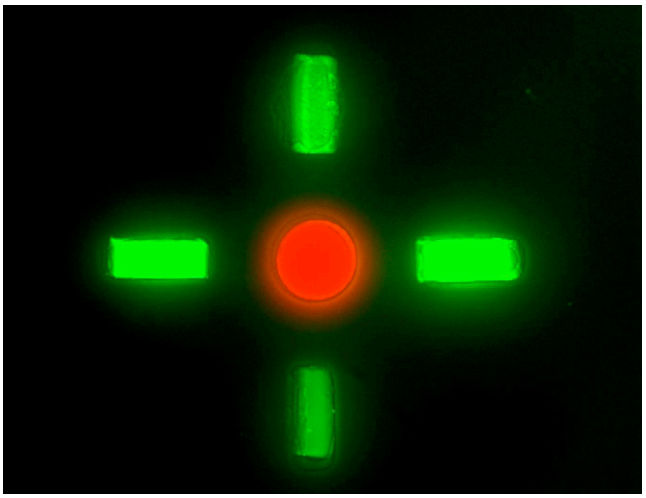

Movie S1. Time lapse of diffusion of fluorescent dyes to measure gradients formed over time within GelMA gels. The circles were dosed with 100 μg/mL Texas Red-tagged 10-kDa dextran, and the rectangles were dosed with 100 μg/mL Alexa 488-tagged 10-kDa dextran. Images were taken every 10 min for 100 min using the same exposure and image settings. The video was recorded at 5 frames per second.

Movie S1

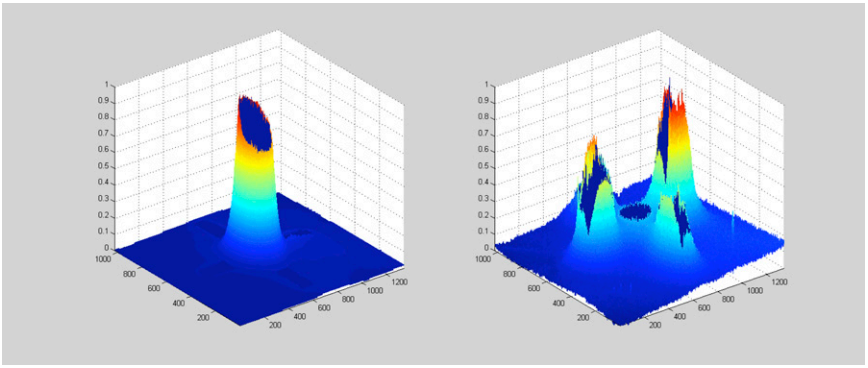

Movie S2. Time lapse of MATLAB-quantified fluorescent intensities formed over time within GelMA gels. The left panel shows normalized red fluorescent intensity and the right panel shows normalized green fluorescent intensity. Each frame is represents images taken 10 min apart. The video was recorded at 5 frames per second.

Movie S2